Structural and Surface Morphology Investigation Of CdSe quantum dots (QD's.)

Prof. Dr. Mohamed Anwar Batal [1] Prof. Dr. Mohamed Amin Al-Baik [2] Rashwan Hamisho [3]

Abstract

Semiconducting quantum dots (QD's) of CdSe were prepared using polar solvents (distilled water and ethylene glycol), and coated with organic capping agent 3-sulfanylpropanoic acid in order to compare the two preparing methods in terms of formed phase by using x-ray diffraction spectra. The core material CdSe QD's was found to be existed in two natural crystal structures: hexagonal structure (wurtzite type) (WZ) and the cubic structure (zinc-blende type) (ZB). The lattice parameters, the distance between two diffracting lattice planes (d), and the average crystallite size of the CdSe QD's (D) were calculated. The strain (η) and the volume of the unit cell V (cm^3), x-ray density of nanocrystals ρ ($g.cm^{-3}$) and the specific surface area S ($cm^2\ g^{-1}$) for both crystal structures has been calculated.

Key words: CdSe QD's, polar solvents, 3−Mercaptopropanoic acid (3MPA), wurtzite (WZ) structure, zinc−blende (ZB) structure.

[(1)]Professor, Department of physics, faculty of science, Aleppo university, Aleppo, Syria.

[(2)] Professor, Department of physics, faculty of science, Aleppo university, Aleppo, Syria.

[(3)]PhD student, Department of physics, faculty of science, Aleppo university, Aleppo, Syria.

دراسة الخصائص البنيوية ومورفولوجيا السطح للنقاط الكمية من CdSe

أ.د.محمد أنور بطل[1] أ.د.محمد أمين البيك[2]
رشوان حميشو[3]

الملخص

تم تحضير نقاط كمية نصف ناقلة (QD's) من CdSe باستخدام مذيبات قطبية (الماء المقطر والإيتيلين غليكول) ومغلفة بعامل التغليف العضوي 3–حمض سلفانيل بروبانويك (3MPA) لمقارنة طريقتي التحضير من ناحية الطور المتشكل، وذلك باستخدام طيف انعراج الأشعة السينية. وُجد أن نويات النقاط الكمية من CdSe تتواجد في بنيتين بلوريتين طبيعيين: البنية السداسية (نوع Wurtzite) والبنية المكعبة (نوعZinc–blend). تم حساب معلمات (بارامترات) الشبكة البلورية المسافة بين مستويات الانعراج البلورية (d) ، ومتوسط حجم البلورة للنقاط الكمية من CdSe (D). تم حساب الانفعال (η) وحجم خلية الوحدة (cm^3) V وكثافة الأشعة السينية للبلورات النانوية ($g.cm^{-3}$) ρ ومساحة السطح المحددة (cm^2g^{-1}) s لكل من البنيتين البلوريتين.

الكلمات المفتاحية: النقاط الكمية CdSe QD's ، المذيبات القطبية، حيود الأشعة السينية (XRD)، 3–sulfanylpropanoic acid (3MPA)، البنية السداسية wurtzite (WZ) ، بنية الزنك Zinc blend (ZB).

(1) **أستاذ دكتور – قسم الفيزياء – كلية العلوم – جامعة حلب – حلب – سورية.**

(2) **أستاذ دكتور – قسم الفيزياء – كلية العلوم – جامعة حلب – حلب – سورية.**

(3) **طالب دكتوراه – قسم الفيزياء – كلية العلوم – جامعة حلب – حلب – سورية.**

1- Introduction:

QDs (Quantum dots), also known as colloidal semiconductor nanocrystals, are generally composed of II–VI and III–V groups of table of elements. Semiconductor nanoparticles or quantum dots of several nanometers in diameter containing only hundreds to a few thousand atoms, have received much attention due to the quantum confinement effect, where the surface electrons of the semiconductor crystallites possess size-dependent wave functions [1]. At this dimension, the area to volume ratio of the particles is amplified and the surface atoms become dominant contribution to the physical and chemical properties. These properties possessed by semiconductor nanoparticles are characterized by variability of energy structure or band gap which can be modified by enhanced surface attributes with particle size reduction [2]. Semiconductor nanocrystals quantum dots (QDs) whose radii are smaller than the bulk exciton Bohr radius constitute a class of materials intermediate between molecular and bulk forms of matter [3, 4]. In quantum dots (QDs), the degree of confinement is determined by the diameter of the nanocrystal. This is analogous to the picture of quantum confinement described by the simple model of a particle in a box. As a result, QDs have electronic states of discrete energies as in atoms and molecules [5]. Among numerous

semiconductor materials, cadmium selenide (CdSe) is one of the most versatile quantum dot materials as its emission peak can be anywhere in the visible spectrum which enables its potential applications ranging from solar-light sensitizers to multicolor fluorescent markers in biological systems [6]. It is an n-type, II-VI semiconductor with an exciton Bohr radius of 6 nm and a direct band gap of 1.74 eV at 300°K. The molecular weight of CdSe is 191.37g/mol where Cd is 58.74% and Se is 41.26% [7]. Bulk form of CdSe is not very interesting but CdSe nanoparticles are one of the most interesting semiconductors which many current researches have focused on their characteristics and applications [8]. The core material CdSe exists in two natural crystal structures, namely the hexagonal (wurtzite type) (WZ) structure and the sphalerite cubic (zinc-blende type) (ZB) structure. The hexagonal state is the stable phase while the sphalerite cubic is the metastable state [9]. The difference between the two structures is subtle, both being of tetrahedral coordination, and also the associated total energy difference is small, of the order of few tens of meV/atom. There is a competition between the covalency and the ionicity effects that determines the relative stability of ZB vs WZ structures, with covalency favoring ZB structure and ionicity favoring wurtzite structure. For CdSe, zincblende is the stable low temperature phase and above a critical temperature, it transforms to wurtzite structure[10].

2-The objectives of research

This research aims to use the x-ray diffraction (XRD) analysis to study the nanocrystalline structure of CdSe QD's prepared using different polar solvents, in order to find the most stable and best-growing phase by calculating the most important lattice constants and parameters.

3-Materials and methods of research

3-1- Used devices and equipments

1- X-ray diffraction from Philips company, No. PW 3710.

2-UV – VIS Spectrophotometer from SCINCO company, No. S-3100.

3-2-Synthesis of CdSe QD's.

3-2-1- CdSe quantum dots prepared using distilled water.

CdSe quantum dots were synthesized by following these four steps: First, 25.2 gr of Na_2So_3 (sodium sulfite) was dissolved in 200 ml of distilled water and then put on a `magnetic stirrer for five minutes until the formation of a transparent solution. Second, 7.89

gr of selenium powder is added, turning the solution black. The previous mixture was placed in a three-neck flask and a reversible distillation process was performed. Then the solution has heated at 80 ºC for 8 hours with continuous stirring, while 20 ml of hydrazine hydrate $N_2H_4H_2O$ had added at a rate of 5 ml per hour until a red winey solution of Na_2SeSo_3 has obtained. This compound is called solution (A) and it is placed in the dark. Third, the solution (B) was formed by dissolving 12.6 gr of cadmium chloride $CdCl_2$ in 50 ml of distilled water on a magnetic stirrer using heat (40ºC). The transparent resulting solution is called (B). Finally, 1 ml of solution (B) was mixed with 1 ml of solution (A) to obtain CdSe QDs, i.e. achieving the ratio (1:1) of (Cd:Se). 0.5 ml of 3-mercaptopropionic acid (3MPA) were added to each (2 ml) of the previous samples. 3MPA had used as a capper to stop the growth process of QD's at different times to obtain QD's in different sizes. As it has mentioned above, CdSe nanoparticles were coated with organic capping agent 3-sulfanylpropanoic acid which is often called 3-Mercaptopropanoic acid (3MPA). 3MPA is an organosulfur compound with the formula $C_3H_6O_2S$ that is propanoic acid carrying a sulfanyl group at position 3. It is a bifunctional molecule, containing both carboxylic acid and thiol groups. It is a colorless oil. In this case, some of the 3MPA molecules may depart from the CdSe nanoparticles into the solvent until a dynamic equilibrium is established between the adsorbing and desorbing of

3MPA from the NPs surfaces. The carboxylic group of 3MPA was shown to be largely acid dissociated for pH values higher than 5 by Raman spectral study [11]. Figure (1) shows the CdSe QD capped with 3MPA.

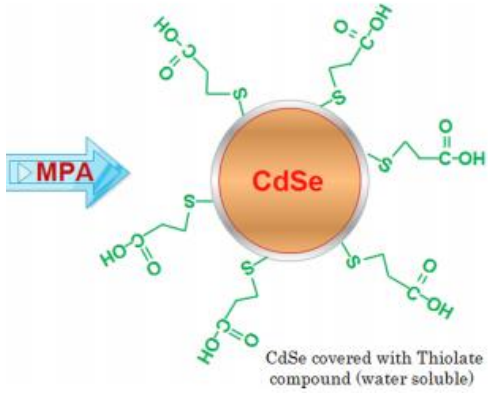

Figure (1) schematic of a CdSe quantum dot (QD) with 3-MPA ligands on the surface.

3-2-2- CdSe quantum dots prepared using ethylene glycol.

The same steps were followed for the CdSe QD's prepared using ethylene glycol by replacing the same amount of distilled water by ethylene glycol $C_2H_4(OH)_2$. Ethylene glycol has used as a solvent and capping agent.

4-Results and Discussion

It has been found that some organic surfactants have a great influence on the structure and phase of nanocrystals. For example,

for CdSe nanocrystals, using trioctylphosphine oxide (TOPO) and trioctylphosphine (TOP) yields the wurtzite phase whereas the use of oleic acid (OA) results in the formation of the zinc blende phase. As these factors change the surface energy, which in turn contributes to the phase stability, so the surface of nanocrystals can exert significant influence on the structures and the properties of nanocrystals . This is because of the differences in surface energies between polymorphs. The theoretical research studied the relative stability which depends mainly on the surface structure of the II–VI compounds. In this work, semiconducting quantum dots of CdSe were prepared using polar solvents (distilled water and ethylene glycol) in order to compare the two preparing methods in terms of formed phase by using x-ray diffraction spectra.

4-1- X-Ray Diffraction (XRD) Measurements

X-ray diffraction (XRD) is a very common and important tool for the characterization of crystal structure properties of QD's such as their phase, inter-planar spacing, and crystalline size by using X-rays. The samples of nanoparticles for XRD analysis were turned to powder by following these steps: Ethanol was added to the samples to precipitate the QD's. The precipitated nanocrystals were separated by centrifugation in a clean centrifuge tube at 7000 rpm for 3 min. Core nanocrystals were cleaned by bathing

them in ethanol then dried at $50^{\circ}C$ for 72 hours. The drying temperature was low and this was substituted by increasing drying time to avoid the QD's growth caused by thermal effect. The phase composition, morphological and the structural properties of the chemically prepared CdSe QD's samples were realistically characterized by using the X-ray diffraction analyses. XRD spectra were recorded at room temperature using Philips PW 1710 diffractometer with CuKα radiation at 40 kV and 30 mA with λ = 1.5406 Å and diffraction angle 2θ from $10°$ to $80°$ to measure the powder X-ray diffraction (PXRD) patterns of the samples. For both CdSe QD's samples (ethylene glycol and distilled water) the step size has been 0.1^{o} and the integration time was 11 seconds. This means that the sampling time typically was around ($70*10*11=7700/3600=2$ hours) for each sample, which is necessary to get good statistics. The measured QD's diameters were 2.62 nm for distilled water and 2.69 nm for ethylene glycol and which calculated using the following experimental expression [3]:

$$D\ (nm) = (1.6122 \times 10^{-9})\lambda^4 - (2.6575 \times 10^{-6})\lambda^3 + (1.6242 \times 10^{-3})\lambda^2 - (0.4277)\lambda + 41.57 \quad (1)$$

Where λ (nm) is the wavelength of the first excitonic absorption peak of the corresponding sample (525 nm for distilled water and 530 nm for ethylene glycol). This means these two types of CdSe QD's are similar in size, which is necessary for minimizing any

differences resulting from size rather than from crystal structure. A typical X-ray diffraction pattern of CdSe/MPA QD's is shown in figure (2). The strong diffraction peaks indicate the formation of well crystallized QD's.

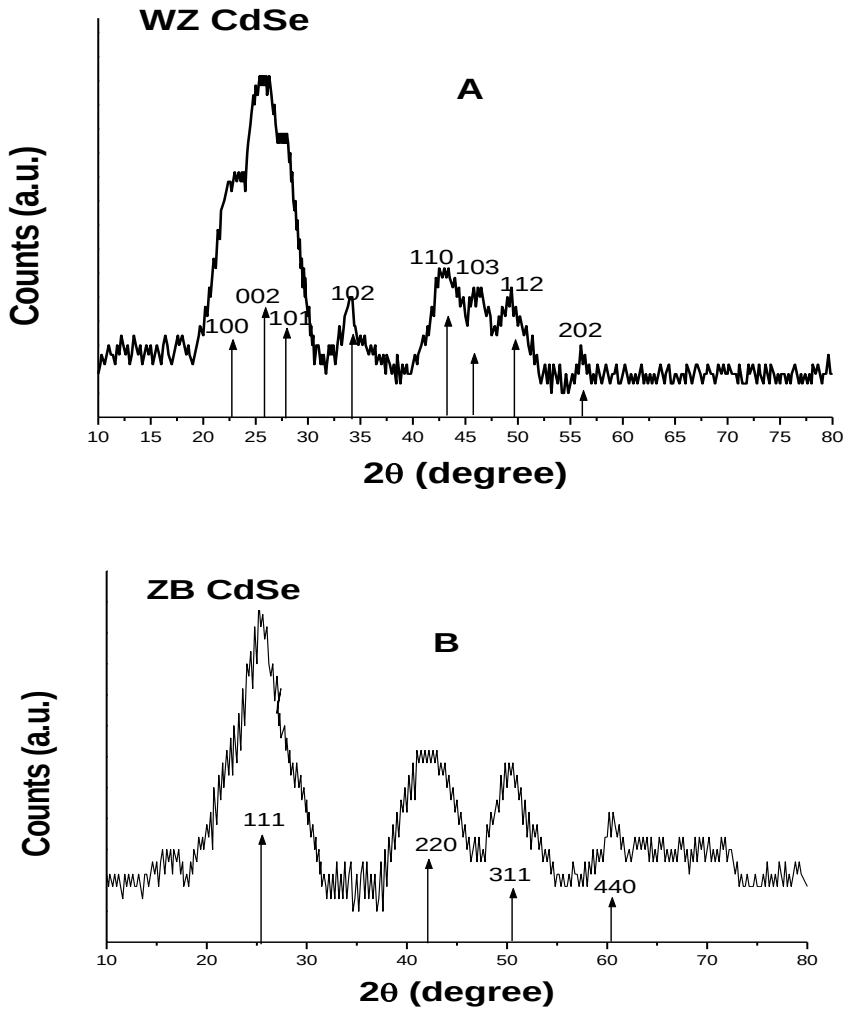

Figure (2) shows the Powder X-ray diffraction patterns (A) for WZ-CdSe QD's (B) for ZB-CdSe QD's.

4-1-1- Phase Determination

The CdSe diffraction patterns exhibit many peak positions corresponding to these of hexagonal wurtzite crystal structure for the sample prepared using distilled water as it showed in figure (2). The peaks obtained at (2θ) angles of 23.09°, 25.5° and 27.59° are correspond to the diffraction lines produced by the (100) (002) and (101) crystal planes, respectively, as identified by standard (JCPDS card No. $04-011-9601$) data. Besides these peaks there are a few other distinct features of the diffract gram obtained at (2θ) angles of 34.13°, 42.9°, 46.06°, 49.44° and 55.98° are correspond to the diffraction lines produced by the (102), (110), (103), (112), and (202) crystal planes, where the clearest ones is a large diffuse signal between 20^{o} and 30^{o}. The XRD pattern clearly demonstrated to the pure hexagonal ($P6_3mc$) phase with wurtzite structure especially for the appearance of the (102) and (103) reflection planes, and also indicates the preferential growth of crystallites in a particular direction of the (002) plane. In addition, it is noticeable that the intensity of (100) and (101) peaks is digressive and that of (002) diffraction peak strengthens, thus the XRD pattern can be indicative of the anisotropic shapes of CdSe sample. For the CdSe QD's sample prepared using ethylene glycol, four diffraction peaks were observed which correspond to a single phase. It was the cubic

($F\overline{4}3m$) zinc blende crystal structure as it shown in figure (2). There were a sharp (1 1 1) peak at 2θ =25.4 °, a deep valley between (2 2 0) peak at 2θ =42.04° and (3 1 1) peak at 2θ =49.74°, as well as a blunt (4 4 0) peak at 2θ =60.91°, and they all imply that the crystal structure here is ZB According to the standard(JCPDS card No. 19-019) data. It can be seen that the major peak (111) is strongly dominating the other peaks because the sample which is crystalline in nature with cubic structure have (111) plane as the preferred growth.

4-1-2- The average particle size Determination

Two elements of similar size, valence, and crystal structure are often miscible enough to form a substitutional solid-solution at any composition. The presence of an atom of a slightly different size distorts the lattice and alters the directions of the diffracted beams. This change in lattice parameter can be determined from the measured d-spacing of diffracting planes. Bragg's law [12] is stated in equation (2), where d is the distance between two diffracting lattice planes (inter plane spacing), λ is the X-ray wavelength (λ = 1.5406 Å); θ is the angle between the X-ray source and the detector and n is the order of the diffraction.

$$2d\sin(\theta) = n\lambda \qquad (2)$$

Table (1) shows the d values corresponding to the diffraction peaks for both WZ and ZB structure.

Table (1) shows the d values corresponding to the diffraction peaks for both WZ and ZB structure

WZ structure			ZB structure		
hkl	2θ of the intense peak (deg)	Inter plane spacing d (Å)	hkl	2θ of the intense peak (deg)	Inter plane spacing d (Å)
100	23.98	3.7378	111	25.4	3.5159
002	25.93	3.5038	220	42.04	2.1508
101	27.09	3.2905	311	49.74	1.8289
102	34.89	2.5752	440	60.91	1.5217
110	42.52	2.1270			
103	45.86	1.9794			
112	49.97	1.8246			
202	55.75	1.6488			

X-ray diffraction peak gets broadens in the nanocrystals due to the crystalline size effect and intrinsic strain effect and this peak broadening normally consists of two parts: physical broadening and instrumental broadening. This instrumental broadening can be corrected using the following relation:

$$\beta_d^2 = \beta_m^2 - \beta_i^2 \qquad (3)$$

Where β_m is the measured broadening, β_i is the instrumental broadening and β_d is the corrected broadening. The average particle size (the mean crystallite size) of the CdSe QD's has calculated in two methods as following.

4-1-2-1- Scherrer method

In this method the instrumental broadening and physical broadening of the sample have been measured as full width at half maximum (FWHM) by taking into account only the crystalline size effect, so the broadening due to size in a particular peak having the (hkl) value can be expressed as:

$$\beta_{FWHM} = \beta_{hkl} = \beta_{size} \qquad (4)$$

Using the size broadening it was possible to calculate the average particle size of the QD's with the help of Scherrer equation [3]:

$$D = \frac{K\lambda}{\beta_{size} .\cos\theta} \qquad (5)$$

In the above expression, the average size of the crystallites is denoted by D (nm), the particle shape factor is k, taken as 0.9 for spherical particles, where λ is the X-ray wavelength of CuK_α radiation (λ = 0.15406 nm), θ is the Bragg diffraction angle and β is the width of the peak at half the maximum intensity of the XRD

peak appearing at the diffraction angle θ in radian. All the previous quantities were calculated and put in table (2).

Table (2) shows the particle size values for both WZ and ZB structure

WZ structure					ZB structure				
hkl	2θ of the intense peak (deg)	FWHM of the intense peak (rad) β	The particle size D (nm)	Average D (nm)	Hkl	2θ of the intense peak (deg)	FWHM of the intense peak (rad) β	The particle size D (nm)	Average D (nm)
100	23.98	0.047	3.015	2.738	111	25.4	0.067	1.366	2.766
002	25.93	0.071	2.002		220	42.04	0.052	1.705	
101	27.09	0.045	3.168		311	49.74	0.046	2.938	
102	34.89	-	-		440	60.91	-	-	
110	42.52	0.058	2.566						
103	45.86	-	-						
112	49.97	0.052	2.941						
202	55.75	-	-						

Hence it can be clearly seen from table (2), that there is a variation in crystallite size of CdSe nanocrystals corresponds to each individual reflection plane may be because of anisotropic growth of samples. By rearranging the above equation, one can write:

$$\cos\theta = \frac{0.9\lambda}{D}.\frac{1}{\beta_{size}} \qquad (6)$$

Now, plotting a graph of $(\cos(\theta))$ versus $(\frac{1}{\beta_{size}})$ known as the Scherrer plot. The average particle size can be calculated from the slope of the graph, but this value won't be correct for many considerations will be explained consequentially.

4-1-2-2- Williamson-Hall analysis

Peak broadening may not only come from the size effect, but can also be due to strain in the particles which affects the diffraction peak positions and width. Scherrer formula considers only the effect of crystallite size on the XRD peak broadening, but it doesn't tell anything about the microstructures of the lattice i.e. about the intrinsic strain, which gets developed in the nanocrystals due to the point defect, grain boundary, triple junction and stacking faults [13]. The W–H analysis is a simplified integral breadth method where strain-induced broadening arises from crystal imperfections and distortion in the lattice. This method demand good data for both high and low angle reflexes . It has therefore been possible to get any information about the strain in the particles. According to which, physical line broadening of X-ray diffraction peak occurs due to the size and micro strain of the nanocrystals, so the total broadening can be written as:

$$\beta_{total} = \beta_{FWHM} = \beta_{hkl} = \beta_{size} + \beta_{strain} \qquad (7)$$

This method considers uniform strain throughout the crystallographic direction, which gets introduced in the nanocrystals due to crystal imperfections. In other words, W–H plot considers strain, which is isotropic in nature. This intrinsic strain actually effects the physical broadening of the XRD profile and this the strain induced peak broadening can be expressed as [14]:

$$\beta_{st\sim ain} = 4\varepsilon\, tan\theta \qquad (8)$$

Where from equation (6), one can write:

$$\beta_{size} = \frac{0.9\lambda}{D}.\frac{1}{\cos\theta} \qquad (9)$$

So, equation (7) can be written as:

$$\beta_{total} = \beta_{FWHM} = \beta_{hkl} = \frac{0.9\lambda}{D}.\frac{1}{\cos\theta} + 4\varepsilon\, tan\theta$$

$$\beta_{hkl}\cos\theta = \frac{0.9\lambda}{D} + 4\varepsilon\, sin\theta \qquad (10)$$

Equation (10) is an equation of a straight line and is known as the uniform deformation model (UDM) equation, which considers the isotropic nature of the crystals. Figure (3) shows the plotting of this equation, with the term ($4\sin\theta$) along X–axis and ($\beta_{hkl}.\cos\theta$) along Y–axis corresponding to each diffraction peak for CdSe

nanoparticles. The slope of this straight line provides the value of the intrinsic strain, whereas the intercept gives the average particle size of the CdSe nanocrystals. The origin of the lattice strain is attributed mainly to the lattice expansion or lattice contraction in the nanocrystals due to size confinement, because the atomic arrangement gets slightly modified due to size confinement, compared to their bulk counterpart. On the other hand, many defects also get created at the lattice structure due to the size confinement and this in turn results in the lattice strain. The average particle size has been determined from the uniform deformation model approximately as 3.18 nm for WZ structure and 2.05 nm for ZB structure. The slope of the UDM plot has been found to be positive for WZ CdSe QD's which indicates the lattice expansion, where it was negative for ZB CdSe QD's which indicates the lattice contraction, and hence in two situation produce an intrinsic strain in the both kind of nanocrystals. From the slope, intrinsic strain has been calculated as 1.11×10^{-3} for WZ and 26.6×10^{-3} for ZB.

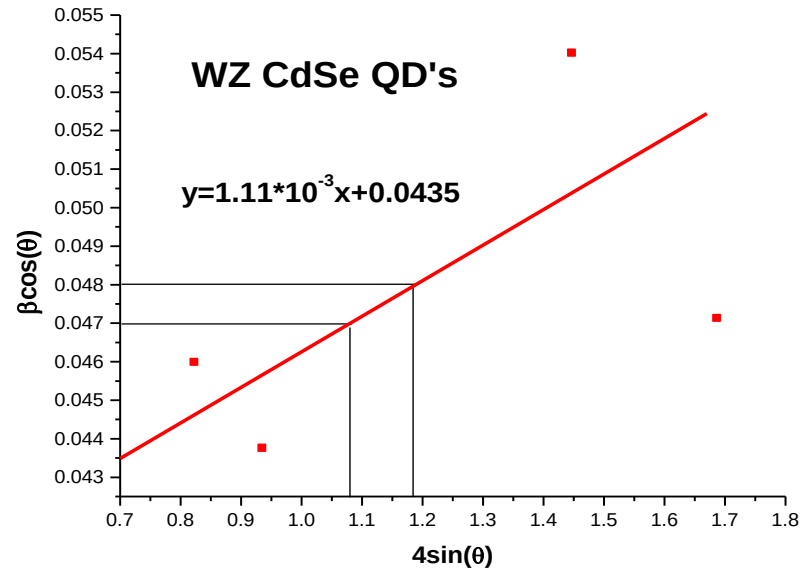

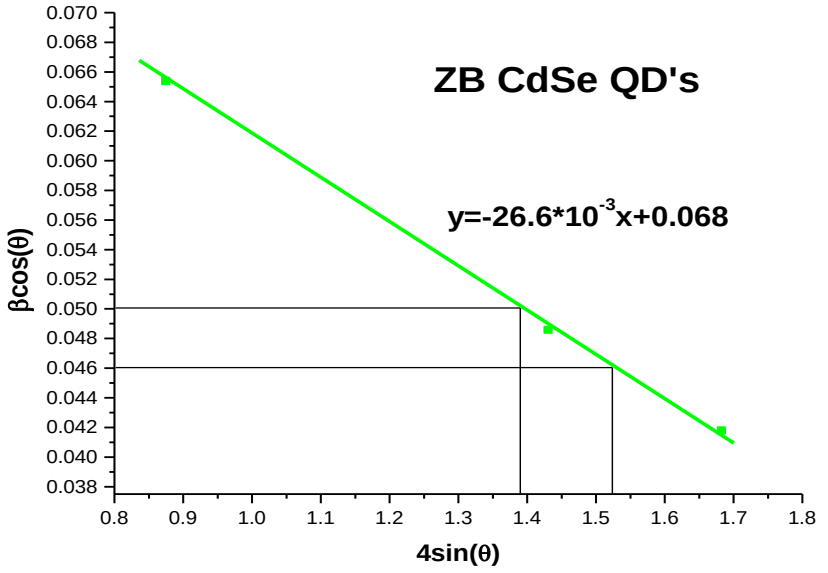

Figure (3) shows the UDM plot for WZ–CdSe and ZB–CdSe QD's.

4-1-2-3- Uniform stress deformation model (USDM)

UDM model is based on the assumption that sample is homogeneous and isotropic in nature, which is not actually justified for a real crystal. Now, as a crystal is anisotropic, Williamson Hall equation should be modified by an anisotropic terms and here for this, an anisotropic strain has been considered. This modified model is the uniform stress deformation model (USDM), where lattice deformation stress has been considered uniform along all the lattice plane directions containing a small micro strain [15]. According to Hooke's law, stress and strain have a linear relationship, where stress is expressed as $\sigma = \varepsilon * Y_{hkl}$, Y_{hkl} being the modulus of elasticity or Young's modulus. So, strain can be expressed as:

$$\varepsilon = \frac{\sigma}{Y_{hkl}} \qquad (11)$$

A small amount of internal stress arises with the intrinsic strain in the crystals due to size confinement. USDM considered stress induced broadening in the XRD peak and anisotropic nature of Young's modulus [16]. Putting the value of ε in equation (10) and on rearrangement, we get:

$$\beta_{hkl}.\cos\theta = \frac{k\lambda}{D} + 4\sigma.\frac{sin\theta}{Y_{hkl}} \qquad (12)$$

This is the modified W–H equation and is known as uniform stress deformation model, which considers the uniform stress in every crystallographic direction. Here, Young's modulus Y_{hkl} can be expressed for hexagonal and zinc blende crystal respectively as [17]:

$$\frac{1}{Y_{hkl}} = (1 - l_3^2)^2 S_{11} + l_3^4 S_{33} + l_3^2(1 - l_3^2)(2S_{13} + S_{44}) \qquad (13)$$

$$\frac{1}{Y_{hkl}} = S_{11} - 2\left[(S_{11} - S_{12}) - \frac{1}{2}.S_{44}\right]\left[\frac{h^2k^2 + k^2l^2 + l^2h^2}{h^2 + k^2 + l^2}\right] \qquad (14)$$

Where l_1, l_2 and l_3 are the direction cosines concerning the a, b and c directions of the crystal lattices, respectively, S_{ij} (S_{11}, S_{12}, S_{13}, S_{33}, S_{44}) are known as elastic compliance constants (the compliance coefficients) of WZ and ZB CdSe and their values are shown in table (3) [17].

Table (3) shows the values of elastic compliance constants Sij for WZ and ZB CdSe QD's

Compliance (S_{ij}) (10^{-11} m^2/N)					
Structure	S_{11}	S_{12}	S_{13}	S_{33}	S_{44}
Wurtzite	2.32	−1.12	−0.55	1.69	7.47
Cubic	3.48	−1.42	−	−	4.48

Using these compliances values, the Young's modulus value have been calculated as it shown in table (4).

Table (4) shows the Young's value corresponding to the reflection planes for WZ and ZB CdSe QD's.

WZ structure			ZB structure		
Reflection planes (hkl)	Young's modulus (GPa)	Average Young's modulus (GPa)	Reflection planes (hkl)	Young's modulus (GPa)	Average Young's modulus (GPa)
100	4.31034	4.845	111	1.9	2.1
002	-		220	2.1	
101	5.91716		311	2.31	
102	-		440	2.1	
110	4.31034				
103	-				
112	-				
202	-				

Plot of equation (12), with the term ($4Sin\theta/Y_{hkl}$) along X-axis and ($\beta_{hkl}.Cos\theta$) along Y-axis corresponding to each peak in the XRD pattern for CdSe nanoparticles, is shown in figure (4). The slope of this plotted straight line provides the value of stress, whereas the intercept gives the average particle size of the CdSe nanocrystals. The average particle size and stress have been determined from the uniform stress deformation model (USDM) approximately as 3.22 nm and 58.82 MPa respectively for the WZ CdSe QD's, while they were 2.02 nm and 95.23 MPa for the ZB CdSe QD's.

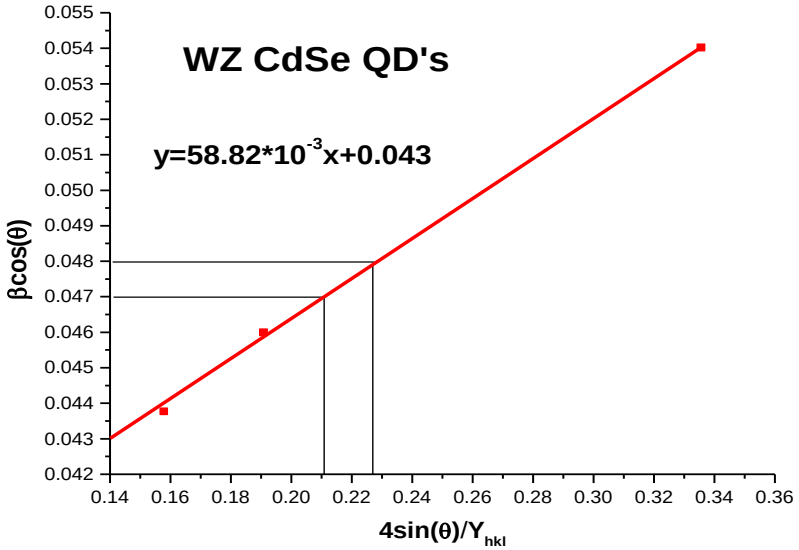

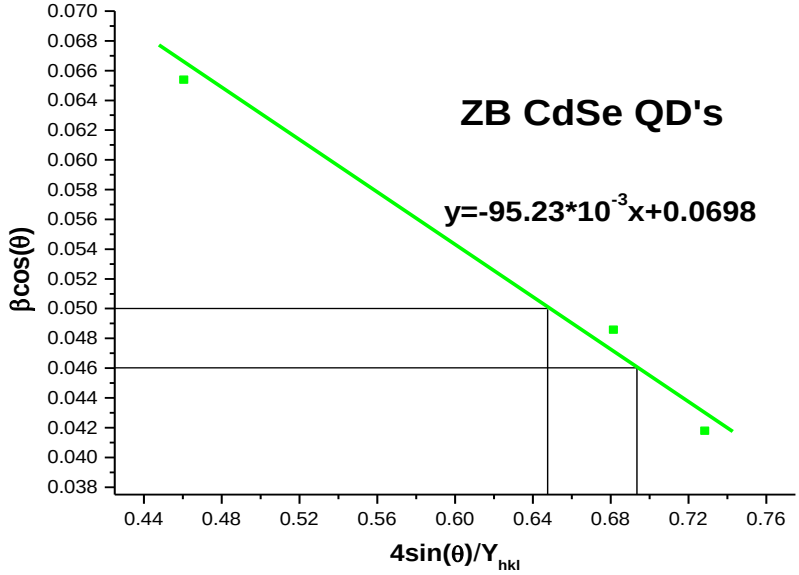

Figure (4) shows the USDM plot for WZ–CdSe and ZB–CdSe QD's.

4-1-2-4-Uniform deformation energy density model (UDEDM)

UDM model assumes the isotropic nature of the crystal, whereas the USDM model assumes a linear relationship between stress and strain, as per Hook's law. But, in real crystals, isotropic nature and linear proportionality between stress and strain, cannot be considered, as because different defects, dislocations, and agglomerates create imperfections in almost all crystals. So, a different model is required, which should be used for the study of the different microstructures of crystals. Here, Uniform deformation energy density model (UDEDM) was used for this purpose, which considers the uniform anisotropic lattice strain in all crystallographic direction and the cause of that uniform anisotropic lattice strain is the density of deformation energy [18]. According to Hooke's law energy density (u) is related to strain with the relation:

$$u = \varepsilon^2 \frac{Y_{hkl}}{2} \qquad (15)$$

Again, we know stress and strain are related as $\sigma = \varepsilon * Y_{hkl}$. So, the intrinsic strain can be written as a function of energy density,

$$\varepsilon = \sigma \sqrt{\frac{2u}{Y_{hkl}}} \qquad (16)$$

Where Y_{hkl} is the Young's modulus. Putting the value of ε in equation (10) and on re-arrangement we get:

$$\beta_{hkl}\cos(\theta) = \frac{k\lambda}{D} + 4\sin(\theta)\sqrt{\frac{2u}{Y_{hkl}}} \qquad (17)$$

Equation (17) is known as the uniform deformation energy density model (UDEDM) equation [19]. From this model, energy density value of the crystals can be calculated as per equation (17). Plot of this equation (17), with the term $(4\sin\theta(\sqrt{2}/Y_{hkl})$ along X-axis and $(\beta_{hkl}.\cos\theta)$ along Y-axis corresponding to each diffraction peak for CdSe nanoparticles, is shown in figure (5). The intercept of the plotted straight line provides the average size as 2.31 nm for WZ and 2.06 nm for ZB, whereas the slope gives the energy density value as 591.36 Kjm^{-3} for WZ and 1084.93 Kjm^{-3} for ZB.

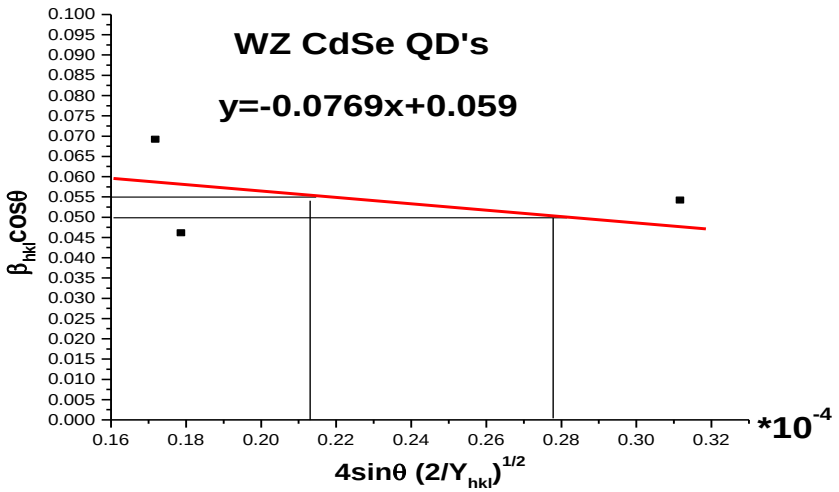

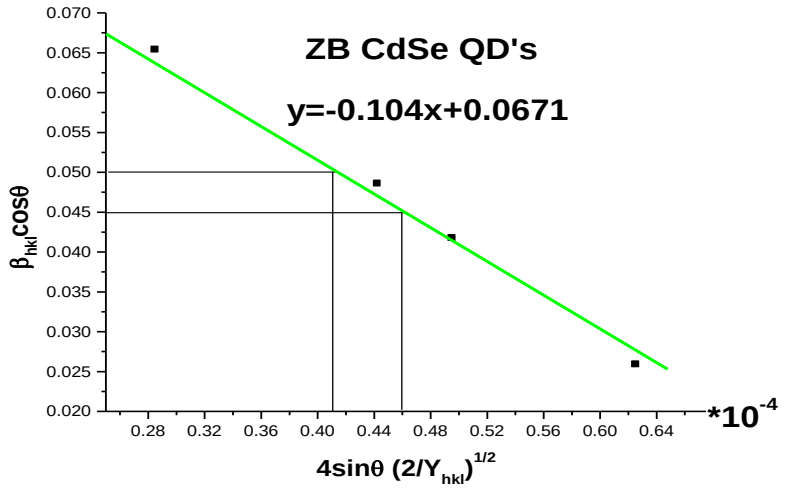

Figure (5) shows the USDM plot for WZ-CdSe and ZB-CdSe QD's.

4-1-2-5- Size-strain plot (SSP)

Williamson-Hall method actually considers the broadening of peaks as a function of diffraction angle (2θ), which is assumed to be combined effect of size induced broadening and strain induced broadening. But there are models, which deals with the peak profile analysis. Size-Strain plot (SSP) is one such method, which considers that XRD peak profile is a combination of Lorentzian function and Gaussian function, where size broadened XRD profile is labelled as a Lorentz function and strain broadened profile is labelled as Gaussian function [20]. So, the total broadening of SSP can be expressed as:

$$\beta_{hkl} = \beta_L + \beta_G \qquad (18)$$

Where β_L and β_G are the peak broadening due to Lorentz and Gaussian function respectively. Further, SSP method always provides a better result for isotropic broadening, as it gives more importance to low angle reflections, where the accuracy and precision are more, than that in higher angles. This is because, at higher angles, XRD data are of lower quality and peaks are generally highly overlapped at higher diffracting angles. So, the SSP calculation is performed using the equation as follow [18]:

$$(d_{hkl}.\beta_{hkl}cos\theta)^2 = \frac{k\lambda}{D}.(d_{hkl}^2.\beta_{hkl}cos\theta) + \frac{\varepsilon^2}{4} \qquad (19)$$

Where d_{hkl} is the lattice distance between the (hkl) planes. Now, using equation (19), a plot is drawn with $(d^2_{hkl} . \beta_{hkl}.Cos\theta)$ term along X-axis and $(d_{hkl}.\beta_{hkl}.Cos\theta)^2$ along Y-axis corresponding to each diffraction peak, which is shown in figure (6). The slope of the straight line provides the average size as 2.1 nm for WZ and 2.31 nm for ZB, whereas the intercept gives the intrinsic strain of the CdSe nanocrystals as $77.45 * 10^{-3}$ for WZ and $97.97 * 10^{-3}$ for ZB.

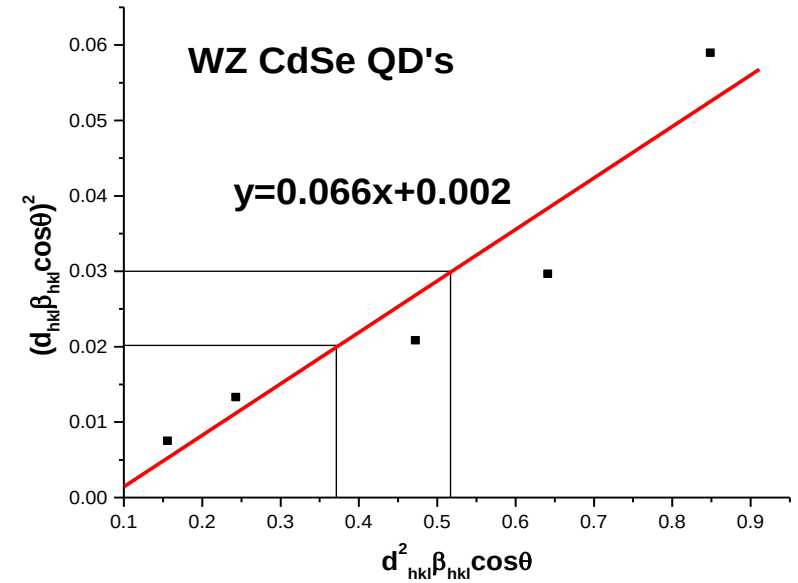

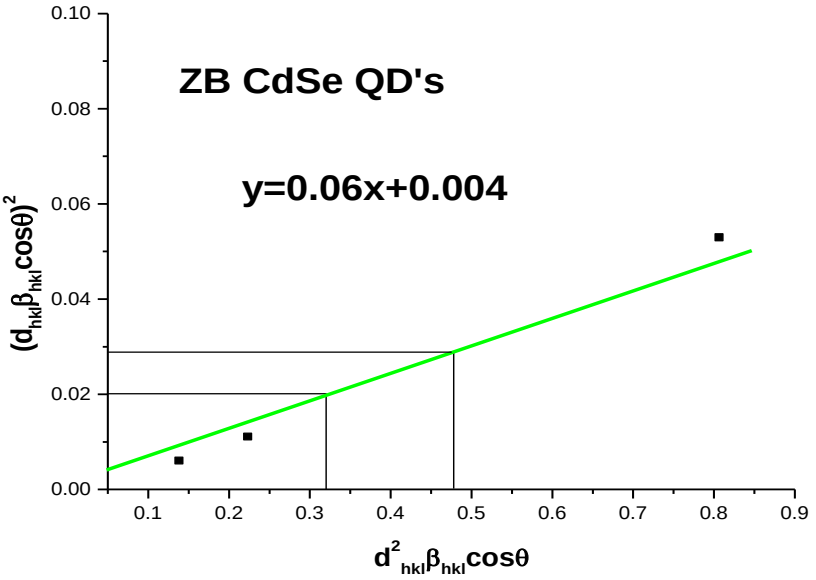

Figure (6) shows the size strain plot for WZ–CdSe and ZB–CdSe QD's

Table (5) shows the particle size values for both WZ and ZB structure in the previous methods.

WZ structure					
D (nm) Optical spectra	D(nm) Sheerer	D (nm) [Williamson-Hall]			
		UDM	USDM	UDEDM	SSP
2.62	2.738	3.18	3.22	2.31	2.1
ZB structure					
D (nm) Optical spectra	D(nm) Sheerer	D (nm) [Williamson-Hall]			
		UDM	USDM	UDEDM	SSP
2.69	2.766	2.05	2.02	2.06	2.31

4-1-3- Lattice Parameter Determination

The cell parameters (lattice parameters), a. b and c for the crystal structure were calculated for both samples of CdSe QD's. For the cubic ZB structure the lattice constant (a=b=c) was calculated by the following relation [21]:

$$a_{cal} = d(h^2 + k^2 + l^2)^{1/2} \qquad (20)$$

For a hexagonal system, like wurtzite there are two lattice parameters a and c, representing the basal and height parameters respectively, and the relation between the lattice spacing d and the miller indices (the lattice plane index) h, k, l and the cell axis a and c (the lattice constants a=b≠c) are given by equation [22]:

$$\frac{1}{d^2} = \frac{4}{3}\left(\frac{h^2 + hk + k^2}{a^2}\right) + \frac{l^2}{c^2} \qquad (21)$$

The lattice parameters were calculated and arranged in table (6) for the both wurtzite and zinc blend structures.

Table (6) shows the lattice parameters for both WZ and ZB structure

WZ structure			ZB structure	
Reflection planes (hkl)	a=b (Å)	c (Å)	Reflection planes (hkl)	a=b=c (Å)
100	4.542	-	111	6.089
002	-	7.007	220	6.082
110	4.25	-	311	6.065

All the previous calculated lattice constants were found to be in very good agreement with the standard data [23]. For the hexagonal WZ structure, the strongest peak (002) was used to estimate the value of lattice constant 'c', while the peaks (100) and (110) were used for the value of 'a=b'. Calculated value of lattice constant (c) is 7.007 Å which is slightly lesser than the standard value 7.010 Å implying that the lattice contraction along c-axis and its value is found to be 0.043%. The average lattice constant 'a=b', on the other hand, calculated 4.396 Å which is slightly larger than the standard value 4.299 Å implying that the lattice expansion in this direction having value 2.206%. It is obvious that when one of the lattice parameters 'c' contract along

c−axis, other lattice constant 'a' will be expanded and vice versa for hexagonal wurtzite system. For very small size of nanoparticles $(2-5)$ nm, surface to volume ratio increases hence most of the atoms reside on their surfaces. Thus lattice of nanoparticles is distorted; it will become contracted or expanded. The volume of the unit cell V (cm^3) for both crystal structures has been calculated using the formula (22), knowing that for cubic ZB structure (a=b=c) and $(\alpha = \beta = \gamma = 90°)$, while in the hexagonal WZ (a=b≠c) and $(\alpha = \beta = 90, \gamma = 120°)$.

$$V = abc\sqrt{1 + 2cos\alpha\ cos\beta\ cos\gamma - cos^2\alpha - cos^2\beta - cos^2\gamma} \qquad (22)$$

This requires that it is for cubic structure, this simplifies to $V = a^3$and for hexagonal it is $V = \frac{\sqrt{3}}{2}a^2c$.

Furthermore, x−ray density of nanocrystals is calculated using the formula [24]:

$$\rho = \frac{\Sigma A}{N_A V} \qquad (23)$$

where ρ is the density of nanocrystals ($g.cm^{-3}$), ΣA is the sum of the atomic weights of all the atoms in the unit cell, N_A is Avogadro's number and V is the volume of the unit cell (cm^3). ΣA = nM, where n is the number of atoms per unit cell and M=191.37

is the molecular weight (a.m.u). Inserting this value in above equation, therefore it takes the following form:

$$\tilde{n} = \frac{nM}{N_A V} \qquad (24)$$

For wurtzite structure of CdSe, the number of atoms per unit cell is considered tow, while it is four for zinc blend. The calculated value of x-ray density where mentioned in table (7). Moreover, the specific surface area (surface free area) of CdSe nanocrystals along the strongest plane is calculated using following formula [24].

$$S = \frac{6}{D.\rho} \qquad (25)$$

Where ρ is x-ray density and D is the crystallite size corrected by SSP Plot (2.1nm for WZ and 2.31nm for ZB) of CdSe nanocrystals, respectively. The values of specific surface area were put in table (7). As the surface area increases surface energy will also be increased hence a higher number of active surface sites are produced.

Table (7) shows the lattice parameters for both WZ and ZB structure

	WZ structure	ZB structure
Lattice constant (Å)	a=b=4.396, c=7.007	a=b=c=6.071
V (cm^{-3}) $\times 10^{-24}$	117.267	224.533
ρ ($g.cm^{-3}$)	4.93	5.652
S ($cm^2.g^{-1}$) $\times 10^7$	0.579	0.459

5-Conclusions and recommendations

The core material CdSe was found to be existed in two natural crystal structures, namely the hexagonal (wurtzite type) (WZ) structure for the samples prepared using distilled water and the cubic (zinc-blende type) (ZB) structure for the samples prepared using ethylene glycol. Scherrer method was followed to calculate the instrumental broadening and physical broadening of the sample have been measured as full width at half maximum (FWHM) by taking into account only the crystalline size effect. Then the values were corrected using W–H analysis method where strain-induced broadening and caused by crystal imperfections and distortion in the lattice. At first the uniform deformation model (UDM) equation had been used, which considers the isotropic nature of the crystals. Then, as a crystal is anisotropic, Williamson Hall equation should be modified by an anisotropic terms, hence, an anisotropic strain has been considered and the uniform stress deformation model (USDM). Finally, Uniform deformation energy density model (UDEDM) was used, which considers the uniform anisotropic lattice strain in all crystallographic direction. The lattice parameters were calculated and were found to be in very good agreement with the standard data.. So many parameters in so many growth conditions still not calculated for both WZ and ZB structures.

References

[1] Salem A, Saion E, Al-Hada N, Kamari H, Shaari A, 2017 Synthesis and characterization of CdSe nanoparticles via thermal treatment technique, **Results in physics**, Vol 7 1556-1562.

[2] Alswata A, Al-Hada N, Kamari H, Hussein M, Ibrahim N, 2017 Preparation of zeolite/zinc oxide nanocomposites for toxic metals removal from water, **Results in physics**, Vol 7 723-731.

[3] Gadalla A, Abd El-Sadek M, Hamood R, 2019 Synthesis and optical properties of CdSe/CdS core/shell nanocrystals, **Materials Science-Poland**, Vol 37 149-157.

[4] Mansur S, 2010 Quantum dots and nanocomposites, **Wiley Interdisciplinary Reviews: Nanomedicine and Nanobiotechnology**, Vol 2 113-129.

[5] Ekimov A, Hache F, Schanne-Klein M, D. Ricard, C. Flytzanis, I. Kudryavtsev, T. Yazeva, A. Rodina and A. L. Efros 1994 Absorption and intensity-dependent photoluminescence measurements on CdSe quantum dots: assignment of the first electronic transitions: erratum, **JOSA B**, Vol 11 524-524.

[6] Park J, Lee K, Galloway J, Searson P, 2008 Synthesis of cadmium selenide quantum dots from a non-coordinating solvent: growth kinetics and particle size distribution, **The Journal of Physical Chemistry C**, Vol 112 17849-17854.

[7] Phukan P, Saikia D, 2013 Optical and structural investigation of CdSe quantum dots dispersed in PVA matrix and photovoltaic

applications, **International Journal of Photoenergy**, Vol 2013 1-6.

[8] Nedelcu G, 2008 The heating study of two types of colloids with magnetite nanoparticles for tumours therapy, **Digest Journal of Nanomaterials and Biostructures**, Vol 3 99-102.

[9] Asogw P, 2010 Optical and structural properties of chemical bath deposited CdSe nanoparticle thin films for photovoltaic applications, **Journal of Non-Oxide Glasses**, Vol 2 183-189.

[10] Fedorov V, Ganshin V, 1991 Determination of the Point of the Zincblende-to-Wurtzite Structural Phase Transition in Cadmium Selenide Crystals, **physica status solidi (a)**, Vol 126 5-7.

[11] Fischer F, 2002 3-Mercaptopropionic acid (3-MPA), **Synlett**, Vol 2002 (08) 1368-1369.

[12] Li F, Jin L, Xu Z, Guo Z, 2009 Determination of three-dimensional orientations of ferroelectric single crystals by an improved rotating orientation x-ray diffraction method, **Review of Scientific Instruments**, Vol 80 (8) 085106.

[13] R. Das, S. Sarkar, Determination of intrinsic strain in poly(vinylpyrrolidone)-capped silver nano-hexapod using X-ray diffraction technique, **Curr. Sci**. 109 (4) (2015) 775–778

[14] Hall W, 1949 X-ray line broadening in metals, **Proc. Phys. Soc. Sect. A**, Vol 62 741-743.

[15] DAS R, Sarkar S, 2018 Determination of structural elements of synthesized silver nano-hexagon from X-ray diffraction analysis,

Indian Journal of Pure & Applied Physics (IJPAP), Vol 56 765-772.

[16] Deligoz E, Colakoglu K, Ciftci Y, 2006 Elastic, electronic, and lattice dynamical properties of CdS, CdSe, and CdTe, **Physica B: Condensed Matter**, Vol 373 124-130.

[17] Qin H, Luan X, Feng C, Yang D, Zhang G, 2017 Mechanical, thermodynamic and electronic properties of wurtzite and zinc-blende GaN crystals, **Materials**, Vol 10 1419.

[18] Mote V, Purushotham Y, Dole B, 2012 Williamson-Hall analysis in estimation of lattice strain in nanometer-sized ZnO particles, **Journal of Theoretical and Applied Physics**, Vol 6 (1) 6.

[19] D. Balzar, H. Ledbetter, Voigt-function modeling in fourier analysis of size- and strain-broadened X-ray diffraction peaks**, J. Appl. Crystallogr**. 26 (1) (1993) 97–103.

[20] Dey P, Das R, 2018 Effect of silver doping on the elastic properties of CdS nanoparticles, **Indian Journal of Physics**, Vol 92 (9) 1099-1108.

[21] Barman J, Borah J, Sarma K, 2008 Effect of pH variation on size and structure of CdS nanocrystalline thin films, **Chalcogenide Lett**, Vol 5 265-271.

[22] Parkin I, 2000 Basic Solid State Chemistry Anthony R. West 2nd edn. John Wiley & Sons, Chichester, 1999 xvi+ 480 pages.£ 24.95 ISBN 0-471-98756-5 (pbk), **Applied Organometallic Chemistry**, Vol 14 227-228.

[23] Grosso G, Parravicini G, 2014-**Solid state physics**. Elsevier, 2nd Edtion. Amsterdam, 872p.

[24] Ghasemi A, Davarpanah A, Ghadiri M, 2012 Structure and Magnetic Properties of Oxide Nanoparticles of Fe-Co-Ni Synthesized by Co-Precipitation Method, **International Journal of Nanoscience and Nanotechnology**, Vol 8 207-214.